

# Advanced Mass Spectrometry Techniques for the Structural Characterisation of Supramolecules and Coordination Compounds

Niklas Geue\*

*Michael Barber Centre for Collaborative Mass Spectrometry, Manchester Institute of Biotechnology, Department of Chemistry, The University of Manchester, 131 Princess Street, Manchester, M1 7DN, UK.*

Corresponding author: [niklas.geue@manchester.ac.uk](mailto:niklas.geue@manchester.ac.uk)

## Abstract

Mass spectrometry is routinely used for myriad applications in clinical, industrial, and research laboratories worldwide. Developments in the areas of ionisation sources, high-resolution mass analysers, tandem mass spectrometry, and ion mobility have significantly extended the repertoire of mass spectrometrists, however for coordination compounds and supramolecules, mass spectrometry remains underexplored and arguably underappreciated. Here, I aim to guide the reader through different tools of modern mass spectrometry that are suitable for larger inorganic complexes. I will discuss all steps, from choosing the right technique(s), over sample preparation and technical details to data analysis and interpretation. The main target audience of this tutorial are synthetic chemists and technicians, as well as mass spectrometrists with little experience in characterising labile inorganic compounds.

## 0. Introduction

Mass spectrometry (MS) has emerged as an integral part of the analytical toolbox and is one of the most routinely used techniques. It has been historically well explored for small organic compounds, as such molecules only contain covalent bonds and are mostly easy to ionise.<sup>1</sup> In the last decades, the focus of MS has expanded rapidly, and two areas have shown particularly big promise: the analysis of complex mixtures, e.g. in “omics”,<sup>2,3</sup> and the structural characterisation of biomacromolecules in their native state.<sup>4,5</sup>

Between the extremes of small (organic) molecules and biomacromolecules, the analysis of synthetic inorganic molecules is of particular interest to chemists, including non-covalently bound supramolecules and labile coordination compounds. These systems have become increasingly important in application areas such as medicine, catalysis, materials and in mimicking the functionality of biomolecules.<sup>6</sup> The structural characterisation of such assemblies is challenging, as X-ray crystallography, NMR spectroscopy or computational methods are often difficult or not feasible for larger structures.<sup>6</sup>

Methods adapted from native MS offer a range of advantages for their characterisation over other methods: a) an ultra-high mass resolution, that enables the unambiguous identification of composition and stoichiometry,<sup>5</sup> b) the robust analysis of complex product mixtures, where different compounds are separated by their  $m/z$ , c) the hyphenation with other techniques such as chromatography,<sup>7,8</sup> ion mobility<sup>9,10</sup> or spectroscopy<sup>11,12</sup> and d) the potential to adapt characterisation workflows to an industrial scale if appropriate.<sup>6</sup> The characterisation of supramolecular and coordination compounds using MS has been reviewed regularly,<sup>6,13–23</sup> however, it is still not commonly and confidently used in synthetic laboratories.

This tutorial will focus on the practical application of MS for such inorganic complexes, beginning with technical details as well as potential challenges. The analysis of MS data will further be discussed in detail, before the tutorial ends with an introduction to other gas phase techniques suitable for the investigation of such compounds. While the characterisation of these inorganic systems with MS is less trivial than for small organic compounds, every mass spectrometrist, chemist and technician can learn the necessary skills with the help of this tutorial.

## 1. Technical Details

The main aim of the mass spectrometric analysis is to obtain a mass spectrum of the synthetic reaction product. In this section, I will focus on technical details to facilitate this process and on pitfalls to avoid (Figure 1).

### 1.1 Sample Preparation

Synthetic products are usually provided as solids or as reaction mixtures in solution, and the most common ionisation methods start from solution. For solid samples, the choice of solvent

is crucial. As it is challenging for a mass spectrometrists or technician to understand the intrinsic properties of the synthetic product on the same level as the synthetic chemist, ideas for solvent choices are a valuable input that should be provided. Suitable solvents entirely depend on the reaction product and its properties – the sample (and potentially the ionisation reagent) need to be dissolved easily while maintaining suitable concentrations, but without inducing unwanted disassembly reactions. For labile compounds, it is often advisable to prepare the solution fresh prior to analysis, which minimises the time for disassembly or other reactions. It is also important to choose a solvent that is compatible with the ionisation method of choice. For electrospray ionisation (ESI), this usually involves polar solvents such as water, methanol and acetonitrile, whereas non-polar solvents are less suitable.<sup>28</sup>

For ESI it is often useful to add salts such as alkali metal halides, or acids/bases, depending on the product and its lability. This approach can help to enhance the signal of adduct ions  $[M + x A]^{x+}$  and  $[M + y A]^{y-}$  (with  $A^+/A^-$  being e.g. an alkali metal cation or halide anion), or of the protonated and deprotonated species  $[M + x H]^{x+}$  and  $[M - y H]^{y-}$ , respectively. Buffer solutions to control the pH value, such as ammonium acetate, which are often used in biological mass spectrometry, are usually not needed.<sup>29</sup>

The analyte concentration in solution is important, and this is particularly difficult to control when a reaction mixture is the starting point rather than a solid. Modern mass spectrometers are increasingly sensitive and the optimal sample concentration is decreasing constantly.<sup>30</sup> Typical analyte concentrations in modern MS lie in the low  $\mu M$  region.

*What are the consequences of using too high concentrations?* One problem is that higher concentrations can cause crystallisation in the solution and at the air/water interface, and when using ESI and nano-electrospray ionisation (nESI), this can often clog the capillary.<sup>31,32</sup> High concentrations also lead to clustering during the ESI process, and this makes the spectrum more complex and may also not reflect the molecules present in solution.<sup>19</sup> Another potential problem are space-charging effects, which are due to the repulsion of charged ions with the same polarity. This phenomenon can lead to a decrease in accuracy, sensitivity and resolution of the mass<sup>33,34</sup> (and ion mobility<sup>35,36</sup>) measurements, although in practice this is often not a problem for mass. High concentrations lead more likely to oversaturation of the detector,<sup>37</sup> which decreases their lifetime, and also means that instruments have to be cleaned more frequently due to the contaminations with neutrals from solution.<sup>22</sup>

What are the consequences of using too low concentrations? Below a certain threshold, the sensitivity of mass spectrometers is not sufficient to detect the analyte. Less obvious is that the formation of coordination compounds and supramolecules is often directed by self-assembly, and this is driven by entropy that in turn depends on concentration.<sup>22</sup> Hence, synthetic products can disassemble in solution because the concentration is too low. Most MS efforts are pointless if the analyte is not present in solution, and for some compound classes, the consequences of using high concentrations have to be accepted in order to maintain the analyte in solution. For metallosupramolecular complexes, typical solution concentrations to avoid disassembly are in the high  $\mu\text{M}$  and low  $\text{mM}$  region.<sup>22</sup>

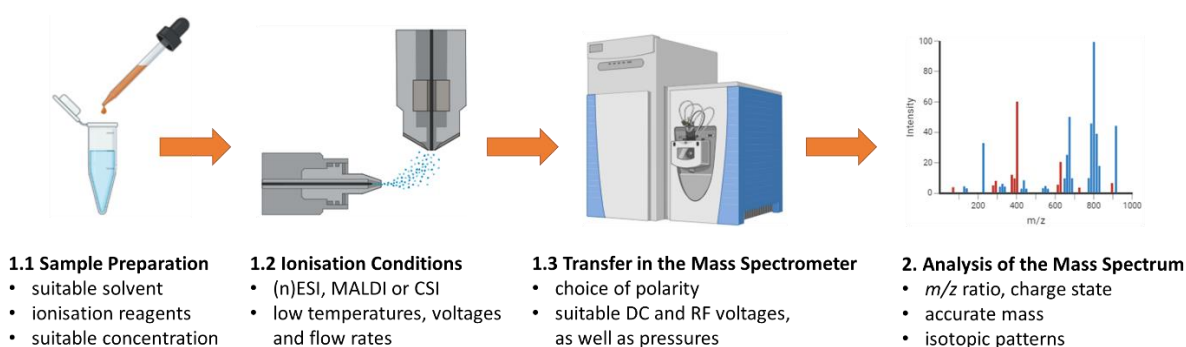


**Figure 1:** Mass spectrometric analysis of supramolecules and coordination compounds, including sample preparation, ionisation conditions, ion transfer and analysis. Designed with BioRender.

## 1.2 Ionisation

The use of soft ionisation methods has significantly improved the characterisation of large biomacromolecules,<sup>38</sup> and the lessons learned from biological MS can be applied to labile inorganic substances.<sup>6</sup> The most commonly used ionisation source is electrospray ionisation (ESI), where a high voltage is applied to a solution in a capillary. Ions in the liquid migrate to the surface until coulombic repulsion overcomes the surface tension and an ion-solvent cone forms at the tip of the capillary. The further mechanism of ionisation depends on the size and structure of the molecule and remains debated.<sup>39–41</sup>

A further improvement over ESI for the ionisation of labile complexes to the gas phase is nano-ESI,<sup>42</sup> for which glass capillaries with a sharp opening in the (sub)micron regime are used.<sup>43</sup> Due to lower flow rates and voltages, and the possibility of lower source temperatures, very large structures such as whole viruses can be ionised, and hence no relevant, upper mass limit

exists for synthetic chemists.<sup>44</sup> The design of these “nano-tips” needs some consideration, and depending on usage, either the purchase of premade nano-tips or the in-house design with capillary pullers is possible. Parameters for common nano-ESI tips can be found elsewhere.<sup>43,45</sup>

For successful ionisation using nESI, a voltage needs to be applied to the solution inside the tip. Two common options exist: the insertion of an inert metal wire (often Pt) that is connected to the source, or the coating of the nano-tip with a conductive material (often Au, Pd or Pt).<sup>46,47</sup> For most cases, both methods are equivalent. The disadvantage of nESI compared to ESI is the difficulty to hyphenate the technique with liquid chromatography, although this has been partially overcome,<sup>48</sup> and a tedious tip preparation. Nano-tips are also not perfectly reproducible, which can make the development of robust workflows difficult.<sup>43</sup>

Source conditions for labile inorganic complexes need to be soft, which means to avoid in-source fragmentation and to preserve the structure of the analyte. Low flow rates, temperatures and voltages are recommended.<sup>22</sup> There is a trade-off between these soft parameters and those that maximise signal (high flow rates, temperatures and voltages), and finding the ideal parameters may require careful tuning. A key step in the formation of ions *via* ESI is desolvation, which benefits from high pressures and temperatures in the ion source, and also depends on the solvent.<sup>49</sup> Incomplete desolvation can lead to solvent adducts, which particularly occur with coordinating solvents like acetonitrile.<sup>19</sup>

The source temperature is a major factor for preserving the original structure of labile molecules during ESI. Cryo- or cold-spray ionisation sources (CSI) have been developed, achieving remarkable results that were not amenable with ESI.<sup>50–52</sup> As CSI is not commercially available and only few sources exist, it will not be discussed further.<sup>53,54</sup>

Matrix-assisted laser desorption ionisation (MALDI) is another ionisation technique, which is often deployed for synthetic molecules such as organic polymers<sup>55</sup> and dendrimers.<sup>56</sup> An important difference to ESI is that fewer multi-charged ions are formed, which facilitates data interpretation. The sample is embedded in an organic matrix, and excited with short laser pulses. After the energy absorption through the matrix and relaxation in the crystal lattice, parts of the sample are desorbed and ionised, and transferred to the mass spectrometer.<sup>57</sup> While MALDI has its merit for labile synthetic molecules, it is far less common than ESI. Other

ionization methods, such as electron ionisation, chemical ionisation or field ionisation are even less frequently used, but can be suitable e.g. for organometallic compounds.<sup>58</sup>

### 1.3 Ion Transfer in the Mass Spectrometer

The transfer of ions in the mass spectrometer is realised through a combination of direct current (DC) and alternating radiofrequency (RF) fields.<sup>59</sup> The most important consideration is the polarity of the ion optics, as this determines whether cations or anions are transmitted. The preference for either polarity depends on the nature of the sample, its acidity/basicity and ionisation energy/electron affinity.<sup>60</sup> Biological MS relies overwhelmingly on the positive ion mode, however for synthetic molecules, negative ion mode is also frequently used. MS data collected in negative ion mode are often simpler, but less intense, due to the availability of fewer ionization pathways.<sup>19</sup>

There is a trade-off between high ion transmission (using high voltages and low pressures) and preserving the ion structure (using low voltages and high pressures), and the required “softness” of the parameters depends on the rigidity and stability of the sample. When selecting an ion in a mass analyser in the centre of the instrument (often a quadrupole), labile compounds can yield mass spectra that include fragment ions, although no additional collision energy is applied (see 3.1 Tandem Mass Spectrometry). This suggests fragmentation due to harsh transfer after the mass analyzer, indicating which ion optics need to be tuned softer.

The  $m/z$  also plays an important role in how well ions are transmitted. Higher  $m/z$  ions require higher RF voltages (and lower RF frequencies, but this is usually not user-controlled), but this is not specific for inorganic compounds. More details on tuning mass spectrometers can be found in resources for the specific instruments.<sup>59</sup> As modern mass spectrometers are able to transmit ions in the Megadalton regime (1 Dalton = 1 Da = 1 g·mol<sup>-1</sup>), the size of synthetic compounds is not a limiting factor for ion transfer.<sup>44</sup>

## 2. Analysis of the Mass Spectrum

The measurement of the mass to charge ratio ( $m/z$ ) is realised in the mass analyser. The three most common mass analysers utilised in modern, commercial mass spectrometers are quadrupoles, time-of-flight (TOF) analysers and ion traps, in particular the orbitrap.<sup>1</sup>

Quadrupoles have the lowest resolution of the ones listed above, and are mainly used for  $m/z$ -selection in tandem mass spectrometry experiments or when only a narrow  $m/z$ -window is sufficient for analysis. Both TOF and orbitraps have significantly higher resolution than quadrupoles. In particular the orbitrap has emerged as a game changer in modern mass spectrometry, as it delivers high resolution with moderate costs and effort, and has hence found its way in many research and industry facilities worldwide.<sup>61</sup> More detailed information about mass analysers can be found elsewhere.<sup>1</sup>

## 2.1 $m/z$ and Mass

High-resolution mass spectra provide wide and rich information that go far beyond the comparison of measured mass with predicted molecular weight. For multiply charged ions, the first step is decoupling the mass  $m$  from the charge  $z$ . High-resolution mass spectra of most small ions show isotopic distributions, and the distance  $d$  between two neighbouring isotopic peaks is related to the charge state of the ion *via* the formula  $d = \frac{1}{z}$  (Figure 2a). Based on the charge state of the ion, the mass can easily be determined by multiplying  $z$  with the measured  $m/z$ . This approach works usually well, except for when a limitation in resolution or overlapping peaks occur (Figure 2b). For the former, the resolution in the mass spectrometer may be increased, e.g. by extending the time the ions spend in the orbitrap.<sup>61</sup> Overlapping peaks can be addressed by deconvoluting the different signals, either manually or with software,<sup>62</sup> or by using orthogonal separation approaches such as tandem mass spectrometry and ion mobility. A classic example of overlapping species is the combination of the monomer  $[M + x A]^{x+}$  and its dimer  $[2 (M + x A)]^{2x+}$ , which share the exact same  $m/z$ . The only difference between both ion populations is the distance between the isotopic peaks, however the pattern may not be easy to interpret. Here ion mobility can help, which separates ions based on their size, shape and particularly charge (see 3.2 Ion Mobility Spectrometry).

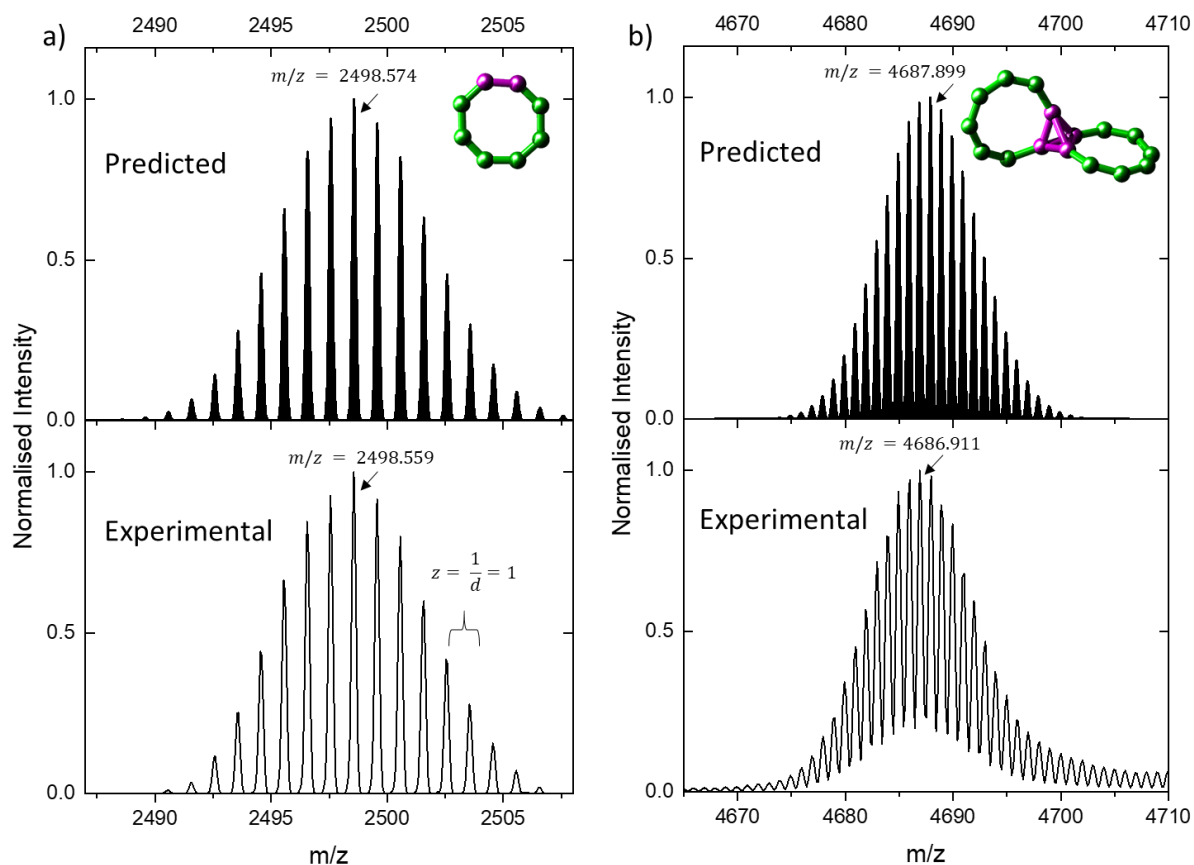


**Figure 2:** Predicted and experimental isotopic pattern of a)  $[Cr_6Gd_2F_8(O_2C^tBu)_{16}NH_2^nPr_2]^+$  and b)  $[Cr_{12}Gd_4F_{21}(O_2C^tBu)_{28}(NH_2^nPr_2)_2]^+$ . Example a) illustrates how the charge state can be determined by quantifying the  $m/z$  distance between two neighbouring isotopic peaks, leading to  $d = z = 1$ . The predicted isotopic pattern agrees well with experiment, and so does the accurate mass of the most intense peak. Case b) is more difficult, and the unexperienced reader might consider the agreement between experiment and prediction sufficient. While the digits of the accurate mass are in good agreement with simulation, the experimental maximum and the whole distribution seems shifted to lower  $m/z$ . The agreement is not sufficient to confidently assign this peak to the proposed sum formula. Based on X-Ray crystallography data, we found that some of the fluoride atoms have likely been substituted for hydroxyl groups, which suggests an overlap of ions with different number of F atoms and OH groups present.<sup>64</sup> a) and b) are simulated with *enviPat*<sup>63</sup> at resolution = 12500.

## 2.2 Resolution and Accurate Mass

Peak overlaps also occur between ions with similar, but not identical  $m/z$ , and for that the resolution of the instrument as well as the accurate mass play an important role. The former defines how well two given peaks can be separated, and continuous advances in commercial instrumentation have led to increasing resolving powers.<sup>65,66</sup>

The accurate mass describes the mass of a given ion more precisely than in integer units. For modern orbitrap and TOF mass spectrometers, these agree with the predicted mass for 1 – 3

digits, depending on the size of the ion, the quality of the calibration and the resolution of the instrument (Figure 2a). It is often not possible for synthetic chemists to recalibrate the instrument, and the mass accuracy can be determined by introducing a sample of known accurate mass (e.g. NaI or CsI clusters) as an internal standard.<sup>19</sup> It can also help to collect a mass spectrum just around the peak of interest, allowing to average as many ions as possible for better accurate mass measurements. The accurate mass can also predict the rough elemental composition of an ion: For molecules that involve only common organic elements such as H, O, N and C, the accurate mass is usually close to the integer ( $\pm 0.2 Da$ ), whereas transition metals often occupy odd accurate masses and their ions are found in the whole range between two integer  $m/z$ .

### 2.3 Isotopic Distribution

High-resolution mass analysers yield isotopic patterns for small molecules, which occur as most elements involve more than one abundant isotope. When many different atoms are combined, their combination yields a fingerprint-like pattern.<sup>19</sup> Based on the ion's sum formula and the natural isotopic abundances for a given element, this pattern can be simulated. Comparison of the experimental and simulated isotopic distribution can guide and confirm the peak assignment to a given formula. For small ions including elements with prominent isotopic distributions (e.g. Cl, S, Fe), the pattern can also reveal how many atoms of an element are present. Several tools are available online to predict isotopic distributions, and software from mass spectrometry vendors also often offers this possibility.<sup>67,68</sup> It is essential to understand that averaged mass spectra, when acquired for a few minutes, can include up to hundreds of millions of ions. With such high ion counts, the statistical foundation of isotopic assignments is very powerful, and an isotopically resolved peak should match the simulated pattern almost perfectly (Figure 2a). The isotopic pattern is also dependent on the instrument and its resolution, and some online resources take that into account.<sup>63,69</sup>

A problem occurs when peaks overlap, which results in a deviation from the expected isotopic distribution (assuming they have similar accurate masses of the isotopic peaks, otherwise they lie in between the other ion's signal). With some experience it is possible to conclude whether a given peak consists of one or more ions, based on peak shape (e.g. whether there is a "valley" in the isotopic distribution), and differences in the accurate mass.

Besides the advantages for peak assignment, the possibility to isotopically resolve peaks also opens a venue for distinguishing a compound from its isotopically labelled species (e.g. with  $^2\text{H}$  instead of  $^1\text{H}$ ). This was for example used by Sawada *et al.* to analyse the preference of different host-guest complex enantiomers.<sup>70</sup>

## 2.4 Analysis Approach

Most users assign the mass spectrum manually, although for frequent users software exists that facilitates this process significantly.<sup>71,72</sup> For any assignment, the  $m/z$ , accurate mass and isotopic distribution need to agree, and the formula needs to be a reasonable guess containing sensible components, oxidation states, coordination numbers and the correct overall charge. I recommend the following procedure for the analysis of a mass spectrum of the molecule M:

1. Search for molecular adduct ions of the formula  $[\text{M} + x \text{A}]^{x+}$  (positive ion mode) or  $[\text{M} + y \text{A}]^{y-}$  (negative ion mode) with one or more charge carrying ions ( $\text{A} = \text{H}^+, \text{Na}^+, \text{K}^+, \text{Cl}^-$  etc.).
2. Look out for other charge states of the same intact analyte, that could originate from different numbers of charge carriers  $\text{A}^+/\text{A}^-$  or through successive loss of oppositely charged counterions.
3. Are there other repeating patterns, separated by the same  $m/z$  ratio? These can indicate cluster formation or polymeric contaminations. Determine the  $m/z$  difference between two neighbouring peaks, and try to assign the pattern. Although these assignments can inform on potential contaminations, it is often more important to avoid them rather than identifying them.
4. If you are unsure if a given peak originates from the analyte or is a contamination in the solvent, run a mass spectrum of the blank. Several contaminant ions are known for ESI-MS, however, often contaminations are sample-specific.<sup>19</sup>
5. Search for reasonable fragments, e.g. for complexes with loosely bound ligands, as well as ions with varying oxidation states of transition metals. These can occur due to reactions with moisture or through electrochemical reactions during ESI.
6. If you find ions with higher masses than M, look for oligomers of M or other aggregates.

7. I recommend trying to assign as many of the intense peaks as possible, however, MS is a highly sensitive technique, and it is easy to get lost in the details of complex spectra. Unless there is a specific ion of interest, I would recommend to assign only analyte peaks that are higher than 10% of the most intense peak. Relative intensities can reflect the composition in solution well, however they are influenced by how easy the molecules ionise and by the ions' stabilities.
8. The peaks that cannot be assigned with steps 1-5 can be subjected to MS<sup>2</sup> (see 3.1 Tandem Mass Spectrometry). Try tracking the fragmentation channels of these peaks down at various collision energies and write down the leaving groups, which will add up to the formula of the original ion.
9. If it is not possible to identify any peak related to M, it is likely necessary to change solution conditions and ionisation/MS parameters as discussed above.

### 3. Two-Dimensional Gas Phase Separation Approaches

#### 3.1 Tandem Mass Spectrometry

Most commercial mass spectrometers can perform tandem mass spectrometry (MS<sup>2</sup>) experiments. In an MS<sup>2</sup> experiment, ion populations are selected based on their  $m/z$  (commonly with a quadrupole), and subsequently activated, which usually results in smaller fragment ions that are in turn mass-analysed. The activation of ions can be realised *via* energetic collisions with inert gas (collision-induced dissociation, CID) or surfaces (surface-induced dissociation); electron- (electron capture or transfer dissociation) or photon-mediated (ultraviolet-photodissociation or infrared multiphoton dissociation), as well as with other methods.<sup>73,74</sup> The most common MS<sup>2</sup> technique is CID, in which ions are accelerated into a collision cell filled with a stationary inert gas (e.g. N<sub>2</sub>, Ar, Xe). After every gas collision, translational energy of the ion is converted to vibrational energy, which is distributed throughout the ion, usually leading to the dissociation of the weakest bonds. Other tandem mass spectrometry activation methods are not widespread or commercially available, and are beyond the scope of this article.<sup>73</sup>

The main information from CID experiments is the composition of fragment ions and indirectly of the leaving groups (fragment mass = precursor mass – leaving group mass), and

the stoichiometries of the fragments can inform on the structural subunits present in the original precursor ion and their connectivities. Fragments can further dissociate to secondary fragments, and it is important to select collision energies appropriately.

The fragmentation of singly charged species occurs from high to low  $m/z$ , involving the loss of neutral leaving groups that lead to singly charged fragment ions. An ion of the structure  $[AB]^+$  can fragment to  $[A]^+$  and the neutral B, or to  $[B]^+$  and A. Both ions  $[A]^+$  and  $[B]^+$  are at lower  $m/z$  than the precursor  $[AB]^+$  (Figure 3). As neutral leaving groups cannot be detected, data visible in the mass spectrum is biased towards structures that maintain charge, which is influenced by their size and structure. For the fragmentation of multiply charged species, the charge state  $z$  can change, leading to fragment ions at higher  $m/z$  (but lower  $z$ ) than the precursor. It is possible that both products of the precursor retain a charge.<sup>19</sup> An ion  $[AB]^{2+}$  can dissociate to  $[A]^+$  and  $[B]^+$ , and due to the reduction of the charge state  $z$ , either (but not both) of these ions can be at higher  $m/z$  than the precursor (Figure 3).

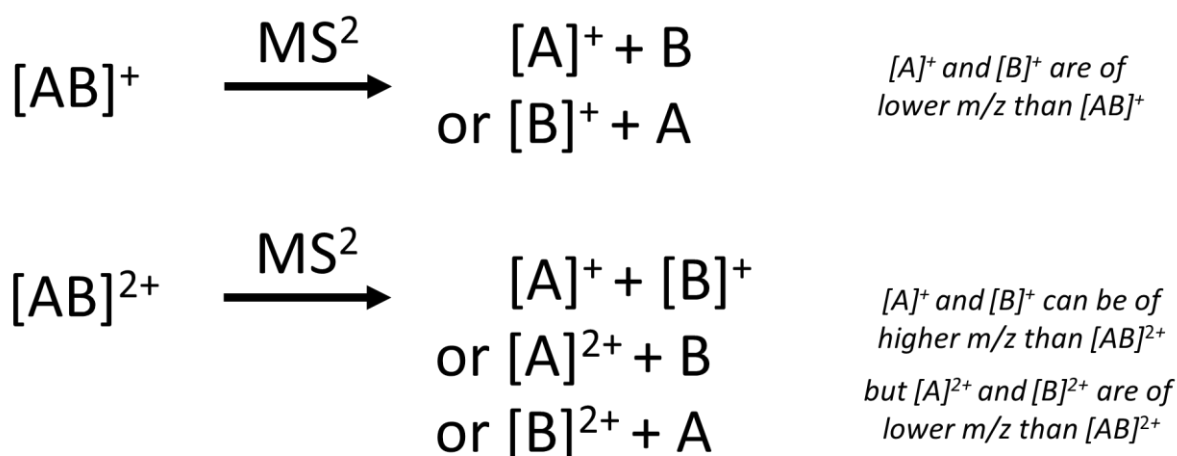


**Figure 3:** Fragmentation of the singly charged  $[AB]^+$  and the doubly charged  $[AB]^{2+}$ . For  $[AB]^+$ , the fragment ions  $[A]^+$  and  $[B]^+$  are found at lower  $m/z$  than the precursor. The dissociation of  $[AB]^{2+}$  can result in  $[A]^+$  or  $[B]^+$  at higher  $m/z$  than the precursor, due to the loss of charge, whereas  $[A]^{2+}$  and  $[B]^{2+}$  are always at lower  $m/z$  than  $[AB]^{2+}$ .

I will now discuss two hypothetical cases consisting of subunits C, D, E, F and X, Y, respectively (Figure 4). These examples are based on the assumption that all subunits cannot dissociate further, and that the ions are equally likely to retain the charge upon fragmentation.

The precursor ion consists of C, D, E and F, and the ions CD, DE, EF, and FG are found in the  $MS^2$  spectrum (Figure 4a top). From this data, it can be derived that C is likely linked to D and

F; D is linked to C and E; E is linked to D and F; and F is linked to E and C. The most sensible explanation is a circular structure of the type CDEF, in which C and F are connected as well, whereas the absence of the ion CF would have indicated a linear connectivity (Figure 4a bottom). Real examples are more complex, and structural rearrangements can occur and need to be taken into account when deriving structural information from MS<sup>2</sup> spectra.<sup>75,76</sup>

Another factor are the relative intensities of fragments, which can inform on two points: 1) *Likely fragments statistically occur more often.* In a chain XYX, the fragments X, Y and XY could be observed (Figure 4b). Fragment Y will likely have the least intense signal at low collision energies, as both X-Y bonds have to be broken. Conversely, both X and XY will occur with similar intensities after the first fragmentation step, as every broken X-Y bond results in equal amounts of X and XY. 2) *Stable fragments are more abundant.* XY is potentially less stable than X as it can dissociate a second time to X and Y, whereas X cannot further fragment. Hence, the relative intensities of the fragments would follow the order X > XY > Y, until at high fragmentation energies XY disappears completely and twice as many X are present relative to Y (Figure 4b).

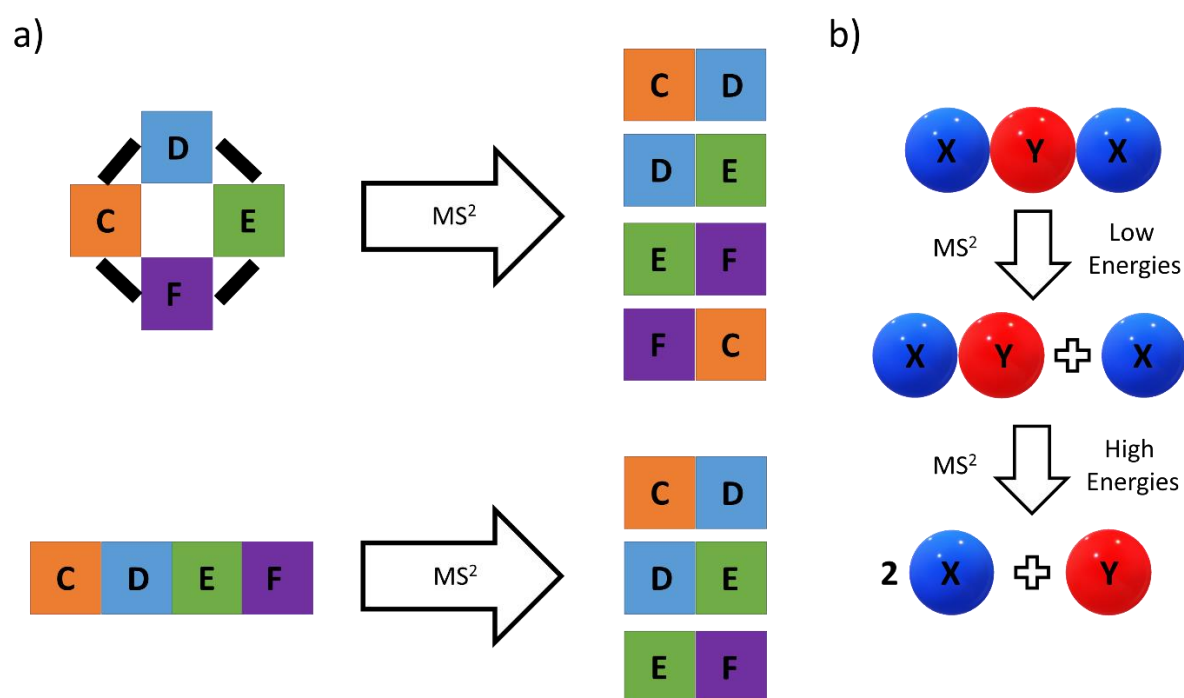


**Figure 4:** a) Fragmentation of CDEF with either a cyclic or linear structure. The presence or absence of CF can inform on the connectivity of CDEF. b) Fragmentation of the chain XYX to the fragments XY + X at lower and 2X + Y at higher collision energies, respectively. The relative abundances of X, Y and XY can inform on the precursor structure.

The appearance of fragment ions is dependent on the collision voltage, which multiplied by  $z$  corresponds to the collision energy  $E_{lab}$ . This energy is user-defined and stable ions require higher collision energies to fragment, and varying the energy can investigate ion structure and stability. A good illustrating example is a host-guest complex, in which the guest is encapsulated into the host. It is also possible to have “*exo*”-coordination of the guest outside the host, for example, when the guest is too large.<sup>25</sup> The host-guest complex will have a higher stability than the *exo*-coordinated compound, and higher collision energies are required to dissociate the non-covalent bonds in the former. This illustrates how MS<sup>2</sup> experiments can distinguish different compounds based on their stabilities.

Stabilities can also be quantified using MS<sup>2</sup> by ramping the collision energy and plotting it against the “survival yield” (SY), which represents the share of precursor ions that does not fragment. These curves are usually S-shaped, and certain points in the fitted graphs can be determined, e.g. the  $E_{50}$  value where 50% of the precursor fragment. These values can be regarded as relative measures of ion stability.<sup>77,78</sup> While they have a thermodynamic meaning for some non-commercial instruments (“guided ion-beam mass spectrometers”),<sup>79</sup> for commercially available platforms these depend on the instrument, pressures, voltages and ion structure. The latter is important as large structures experience more collisions, and this kinetic effect can interfere with thermodynamic properties.  $E_{50}$  and similar values should hence be regarded as semi-quantitative data, which are best used for the interpretation of trends between similar ions, where differences in kinetic effects can assumed to be negligible.

One example from my own research is the fragmentation and stability trend of the polymetallic rings  $[\text{Cr}_7\text{M}^{\text{II}}\text{F}_8(\text{O}_2\text{C}^t\text{Bu})_{16}]^- = [\text{Ring}_{\text{M}}]^-$  (Figure 5a Inset), in which seven Cr<sup>III</sup> and one divalent metal ( $\text{M}^{\text{II}} = \text{Mn}^{\text{II}}, \text{Fe}^{\text{II}}, \text{Co}^{\text{II}}, \text{Ni}^{\text{II}}, \text{Cu}^{\text{II}}, \text{Zn}^{\text{II}}$  and  $\text{Cd}^{\text{II}}$ ) are bridged *via* fluoride and pivalate ligands ( $\text{O}_2\text{C}^t\text{Bu}^-$ ,  $\text{Piv}^-$ ). The dissociation of these anions proceeds through multiple channels, and for  $[\text{Ring}_{\text{Mn}}]^-$  this involves the loss of Mn<sup>II</sup> and two Piv<sup>-</sup> (to **1**), or the loss of Cr<sup>III</sup>, one F<sup>-</sup> and two Piv<sup>-</sup> (to **2**) or three Piv<sup>-</sup> (to **3**) (Figure 5a). The isostructural ions with other M<sup>II</sup> fragment similarly, and as kinetic affects are likely small, differences in the stability curves (Figure 5b) and  $E_{50}$  values are associated with thermodynamic trends. We found  $E_{50}$  differences of up to 22% between the most stable  $\text{M}^{\text{II}} = \text{Ni}^{\text{II}}$  and the least stable  $\text{Cu}^{\text{II}}$ , which we rationalised with trends from crystal field theory.<sup>27</sup>

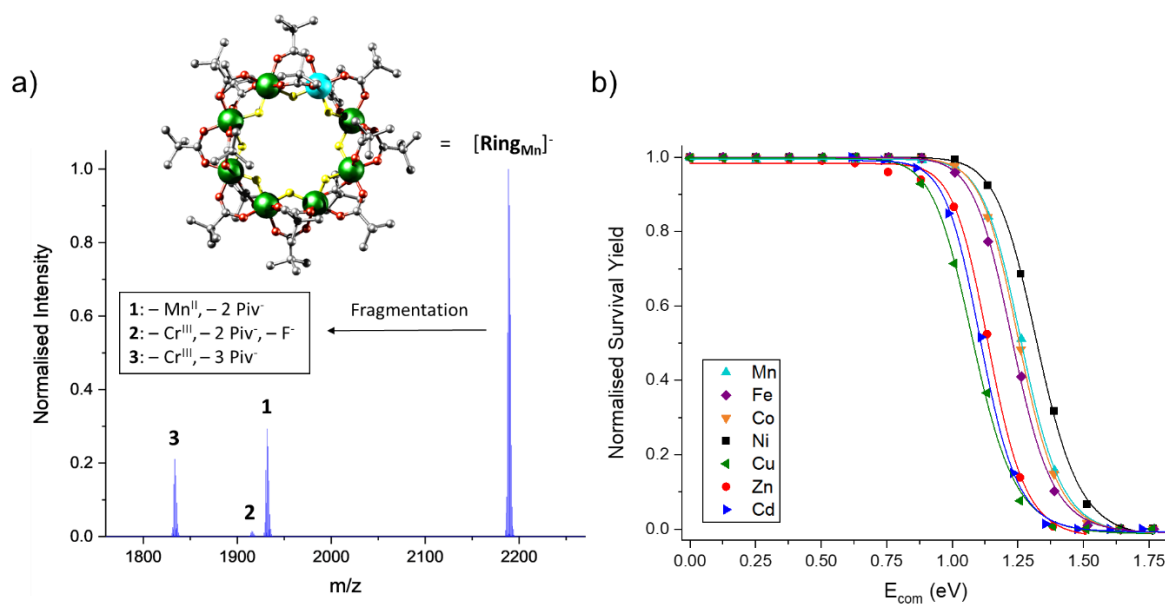


**Figure 5:** (a) MS<sup>2</sup> data of [Ring<sub>Mn</sub>]<sup>-</sup> at E<sub>lab</sub> = 110 eV. Inset: structure of [Ring<sub>Mn</sub>]<sup>-</sup> (Cr: green, Mn: cyan, F: yellow, O: red, C: gray). Hydrogen atoms in the tert-butyl groups were omitted for clarity. (b) Normalized survival yield vs E<sub>com</sub> for [Ring<sub>M</sub>]<sup>-</sup> fitted to a sigmoidal function (M = Mn: cyan, Fe: purple, Co: orange, Ni: black, Cu: green, Zn: red, Cd: blue). E<sub>com</sub> is the collision energy in the center-of-mass frame and is a more precise representation of the energy that is transferred during ion-gas collisions. Reproduced from previous work.<sup>27</sup>

Investigating the stability of compounds is not easily achievable with other techniques, and the unique feature of MS<sup>2</sup> is that solvent molecules and counter ions do not interfere, making it possible to decouple these effects from the actual analyte stability.<sup>6,80</sup> MS<sup>n</sup> experiments (with n > 2) are possible, although not necessarily available in commercial instruments, and this technique can investigate the disassembly and stability of already fragmented ions.<sup>81</sup>

### 3.2 Ion Mobility Spectrometry

Ion mobility (IM) is increasingly used in commercial instrumentation, separating ions based on their size, shape and charge. In the easiest form, ions move through a gas-filled drift cell guided by an electric field. The electric field is usually not strong enough to induce fragmentation, however, collisions with the buffer gas still occur, the more the larger the ion. The collisions determine the time the ion spends in the drift cell, and by injecting ion pulses and measuring this time, structural information is gained. The drift (or arrival) time can be converted to a collision cross section (CCS) value, which is comparable across instruments and to values computationally simulated from candidate geometries (e.g. based on hand-drawn molecular models, density functional theory or molecular dynamics calculations).<sup>9,82</sup> The

community has witnessed a significant increase in the use of IM, however, it is still often limited to expert laboratories. Synthetic chemists and technicians often do not have access to such platforms, and I will hence not discuss this technique in detail.<sup>9,10,80,85</sup>

IM can be particularly powerful when combined with MS<sup>2</sup>, as this enables the structural characterisation of collisionally activated ions and fragments. One historic example I want to briefly mention is the use of IM to distinguish carbon allotropes. The structural evolution of carbon clusters was a hot topic in the 1990s, and different groups independently investigated the formation mechanisms of fullerenes. With an increasing number of carbon atoms, a transition *via* linear chains – monocyclic rings – polycyclic rings – fullerenes was observed through different peaks in IM data.<sup>86,87</sup> It was also shown that collisional activation induces rearrangement from rings to fullerenes, revealing the formation mechanism of the famous Buckminster fullerene C<sub>60</sub>.

The study of the polymetallic rings [Ring<sub>M</sub>]<sup>+</sup> (Figure 5) further illustrates the insights that IM can offer. We coupled MS<sup>2</sup> with IM to measure the size and shape of fragments **1-3** (Figure 6a). For all three species, we found two CCS distributions: one at lower CCS and narrow (**C**, “compact”) and one with a wider peak shape at higher CCS (**E**, “extended”). Based on computational structure optimisations and CCS simulations, we assigned these to closed rings (**C**) and conformationally dynamic, open structures (**E**, Figure 6b).<sup>84</sup> Taken together, these two examples highlight the richness of structural data that can be obtained from IM, and I anticipate that its application in synthetic laboratories and facilities will significantly increase in the future.<sup>80</sup>

[Ring<sub>M</sub>]<sup>+</sup> can encapsulate ammonium cations to form rotaxanes, and I will discuss the case example of the polymetallic rotaxane **Am<sub>Mn</sub>** in the Supporting Information, including sample preparation, MS data analysis, as well as MS<sup>2</sup> and IM measurements and interpretation.

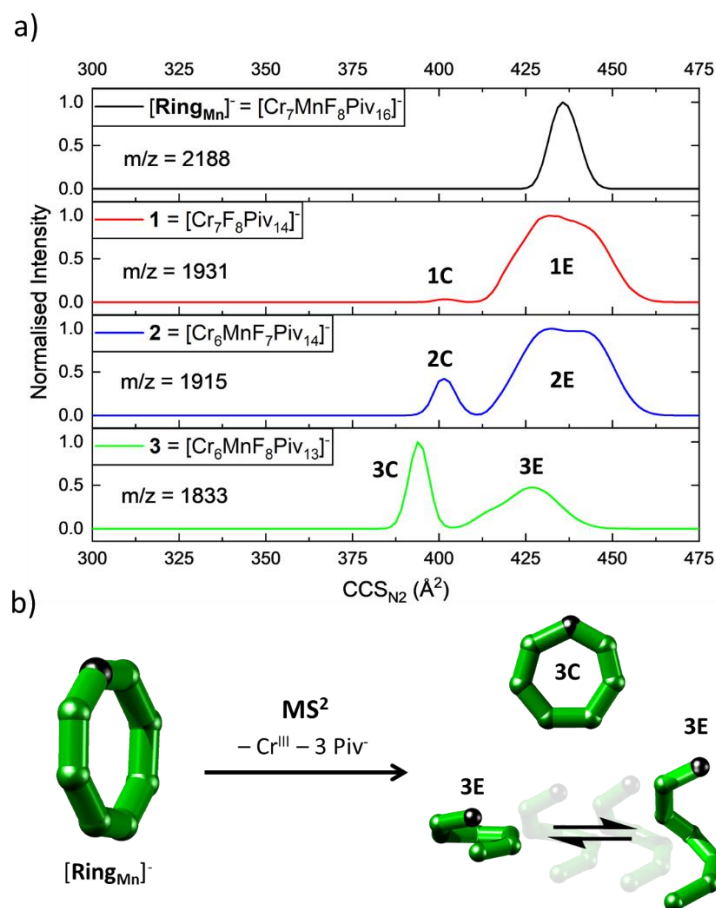


**Figure 6:** a)  $CCS_{N_2}$  Distributions of  $[Ring_{Mn}]^-$  and fragments (1–3) at  $E_{lab} = 110$  eV. b) Fragmentation of  $[Ring_{Mn}]^-$  to **3** including structural assignments of **3C** to closed heptametallic rings and **3E** to conformationally dynamic, open structures. Reproduced from previous work.<sup>27</sup>

## 4. Conclusions

I illustrated how the combination of soft ionisation sources, high-resolution mass analysers and commercially available  $MS^2$  and IM additions, enhance our understanding of coordination compounds and supramolecules. The discussion is limited to techniques that are established and commercially available, however MS is an active field of analytical research, and other methods such as ion spectroscopy<sup>11,12,91</sup> or ion soft-landing including microscopic imaging<sup>92</sup> yield unique structural information as well. I predict that these techniques will gain in importance for supramolecules and coordination compounds. This article should be regarded as a guideline on how to make the most of the MS toolbox for labile inorganic compounds,

and I hope that this tutorial inspires synthetic chemists and technicians to analyse such molecules more frequently and with confidence.

## Conflict of Interests

There are no conflicts to declare.

## Acknowledgements

I would like to thank Prof. Perdita E. Barran and Prof. Richard E. P. Winpenny for supervising and mentoring me during and after my PhD at The University of Manchester, and for giving me access to use instrumentation and samples discussed in this study. Dr. Grigore A. Timco is acknowledged for providing samples discussed in this work. I am also grateful for the support of EPSRC through the strategic equipment award EP/T019328/1, the European Research Council for funding the MS SPIDOC H2020-FETOPEN-1-2016-2017-801406 (to Perdita E. Barran) and an Advanced Grant ERC-2017-ADG-786734 (to Richard E. P. Winpenny). I would also like to thank Dr. Kim Greis, ETH Zürich; Dr. Selena Lockyer, The University of Manchester; and Dr. Hugo Samayoa-Oviedo, Purdue University, for the critical revision of this manuscript.

## Biography

Dr. Niklas Geue is a postdoctoral researcher in the groups of Prof. Perdita Barran and Prof. Richard Winpenny at The University of Manchester, UK. He received his Bachelor degree in Chemistry from Leipzig University in Germany in 2019, before he worked on different projects in Analytical Supramolecular Chemistry at the Pontificia Universidad Católica de Chile, the University of New South Wales in Sydney and the University of California, Los Angeles. He obtained his PhD as a President's Doctoral Scholar from The University of Manchester in 2023, where his project focussed on the use of ion mobility mass spectrometry and tandem mass spectrometry for the characterisation of metallosupramolecular complexes. His postdoctoral work now involves the development of ion soft-landing and microscopic imaging for biomacromolecules and supramolecules. Niklas also serves as a committee member of the British Mass Spectrometry Society (BMSS), a board member of the eLeMeNte e.V. society and as an advisory board member of the Friends of the Chemistry Olympiad in Germany (FChO).

## References

- (1) Hoffmann, E. de; Stroobant, V. *Mass Spectrometry: Principles and Applications*; John Wiley & Sons, 2007.
- (2) Karczewski, K. J.; Snyder, M. P. Integrative Omics for Health and Disease. *Nat. Rev. Genet.* **2018**, *19* (5), 299–310. <https://doi.org/10.1038/nrg.2018.4>.
- (3) Paglia, G.; Smith, A. J.; Astarita, G. Ion Mobility Mass Spectrometry in the Omics Era: Challenges and Opportunities for Metabolomics and Lipidomics. *Mass Spectrom. Rev.* **2022**, *41* (5), 722–765. <https://doi.org/10.1002/mas.21686>.
- (4) Pukala, T.; Robinson, C. V. Introduction: Mass Spectrometry Applications in Structural Biology. *Chem. Rev.* **2022**, *122* (8), 7267–7268. <https://doi.org/10.1021/acs.chemrev.2c00085>.
- (5) Tamara, S.; den Boer, M. A.; Heck, A. J. R. High-Resolution Native Mass Spectrometry. *Chem. Rev.* **2022**, *122* (8), 7269–7326. <https://doi.org/10.1021/acs.chemrev.1c00212>.
- (6) Geue, N.; Winpenny, R. E. P.; Barran, P. E. Structural Characterisation Methods for Supramolecular Chemistry That Go beyond Crystallography. *Chem. Soc. Rev.* **2022**, *51* (1), 8–27. <https://doi.org/10.1039/D0CS01550D>.
- (7) Mondello, L.; Tranchida, P. Q.; Dugo, P.; Dugo, G. Comprehensive Two-Dimensional Gas Chromatography-Mass Spectrometry: A Review. *Mass Spectrom. Rev.* **2008**, *27* (2), 101–124. <https://doi.org/10.1002/mas.20158>.
- (8) Holčapek, M.; Jirásko, R.; Lísa, M. Recent Developments in Liquid Chromatography–Mass Spectrometry and Related Techniques. *J. Chromatogr. A* **2012**, *1259*, 3–15. <https://doi.org/10.1016/j.chroma.2012.08.072>.
- (9) Gabelica, V.; Shvartsburg, A. A.; Afonso, C.; Barran, P.; Benesch, J. L. P.; Bleiholder, C.; Bowers, M. T.; Bilbao, A.; Bush, M. F.; Campbell, J. L.; Campuzano, I. D. G.; Causon, T.; Clowers, B. H.; Creaser, C. S.; De Pauw, E.; Far, J.; Fernandez-Lima, F.; Fjeldsted, J. C.; Giles, K.; Groessl, M.; Hogan, C. J.; Hann, S.; Kim, H. I.; Kurulugama, R. T.; May, J. C.; McLean, J. A.; Pagel, K.; Richardson, K.; Ridgeway, M. E.; Rosu, F.; Sobott, F.; Thalassinos, K.; Valentine, S. J.; Wytenbach, T. Recommendations for Reporting Ion Mobility Mass Spectrometry Measurements. *Mass Spectrom. Rev.* **2019**, *38* (3), 291–320. <https://doi.org/10.1002/mas.21585>.
- (10) Dodds, J. N.; Baker, E. S. Ion Mobility Spectrometry: Fundamental Concepts, Instrumentation, Applications, and the Road Ahead. *J. Am. Soc. Mass Spectrom.* **2019**, *30* (11), 2185–2195. <https://doi.org/10.1007/s13361-019-02288-2>.
- (11) Pereverzev, A.; Roithová, J. Experimental Techniques and Terminology in Gas-Phase Ion Spectroscopy. *J. Mass Spectrom.* **2022**, *57* (5), 1–14. <https://doi.org/10.1002/jms.4826>.
- (12) Stroganova, I.; Rijs, A. M. Ion Spectroscopy Coupled to Ion Mobility–Mass Spectrometry. In *Ion-Mobility Mass Spectrometry: Fundamentals and Applications*; 2021.
- (13) Schalley, C. A. Supramolecular Chemistry Goes Gas Phase: The Mass Spectrometric Examination of Noncovalent Interactions in Host-Guest Chemistry and Molecular Recognition. *Int. J. Mass Spectrom.* **2000**, *194* (1), 11–39. [https://doi.org/10.1016/S1387-3806\(99\)00243-2](https://doi.org/10.1016/S1387-3806(99)00243-2).
- (14) Schalley, C. A. Molecular Recognition and Supramolecular Chemistry in the Gas Phase. *Mass Spectrom. Rev.* **2001**, *20* (5), 253–309. <https://doi.org/10.1002/mas.10009>.
- (15) Henderson, W.; McIndoe, J. S. *Mass Spectrometry of Inorganic and Organometallic Compounds: Tools - Techniques - Tips* | Wiley; 2004.

- (16) Baytekin, B.; Baytekin, H. T.; Schalley, C. A. Mass Spectrometric Studies of Non-Covalent Compounds: Why Supramolecular Chemistry in the Gas Phase? *Org. Biomol. Chem.* **2006**, *4* (15), 2825–2841. <https://doi.org/10.1039/b604265a>.
- (17) Cera, L.; Schalley, C. A. Supramolecular Reactivity in the Gas Phase: Investigating the Intrinsic Properties of Non-Covalent Complexes. *Chem. Soc. Rev.* **2014**, *43* (6), 1800–1812. <https://doi.org/10.1039/c3cs60360a>.
- (18) Qi, Z.; Heinrich, T.; Moorthy, S.; Schalley, C. A. Gas-Phase Chemistry of Molecular Containers. *Chem. Soc. Rev.* **2015**, *44* (2), 515–531. <https://doi.org/10.1039/c4cs00167b>.
- (19) McIndoe, J. S.; Vikse, K. L. Assigning the ESI Mass Spectra of Organometallic and Coordination Compounds. *J. Mass Spectrom.* **2019**, *54* (5), 466–479. <https://doi.org/10.1002/jms.4359>.
- (20) Polewski, L.; Springer, A.; Pagel, K.; Schalley, C. A. Gas-Phase Structural Analysis of Supramolecular Assemblies. *Acc. Chem. Res.* **2021**, *54* (10), 2445–2456. <https://doi.org/10.1021/acs.accounts.1c00080>.
- (21) Lloyd Williams, O. H.; Rijs, N. J. Reaction Monitoring and Structural Characterisation of Coordination Driven Self-Assembled Systems by Ion Mobility-Mass Spectrometry. *Front. Chem.* **2021**, *9*. <https://doi.org/10.3389/fchem.2021.682743>.
- (22) Wang, H.; Guo, C.; Li, X. Multidimensional Mass Spectrometry Assisted Metallo-Supramolecular Chemistry. *CCS Chem.* **2022**, *4* (3), 785–808. <https://doi.org/10.31635/ccschem.021.202101408>.
- (23) Zimnicka, M. M. Structural Studies of Supramolecular Complexes and Assemblies by Ion Mobility Mass Spectrometry. *Mass Spectrom. Rev.* **2023**. <https://doi.org/10.1002/mas.21851>.
- (24) Fernandez, A.; Ferrando-Soria, J.; Pineda, E. M.; Tuna, F.; Vitorica-Yrezabal, I. J.; Knappke, C.; Ujma, J.; Muryn, C. A.; Timco, G. A.; Barran, P. E.; Ardavan, A.; Winpenny, R. E. P. Making Hybrid [n]-Rotaxanes as Supramolecular Arrays of Molecular Electron Spin Qubits. *Nat. Commun.* **2016**, *7*, 1–6. <https://doi.org/10.1038/ncomms10240>.
- (25) Kiesilä, A.; Kivijärvi, L.; Beyeh, N. K.; Moilanen, J. O.; Groessl, M.; Rothe, T.; Götz, S.; Topić, F.; Rissanen, K.; Lützen, A.; Kalenius, E. Simultaneous Endo and Exo Complex Formation of Pyridine[4]Arene Dimers with Neutral and Anionic Guests. *Angew. Chem. Int. Ed.* **2017**, *56* (36), 10942–10946. <https://doi.org/10.1002/anie.201704054>.
- (26) Krueve, A.; Caprice, K.; Lavendomme, R.; Wollschläger, J. M.; Schoder, S.; Schröder, H. V.; Nitschke, J. R.; Cougnon, F. B. L.; Schalley, C. A. Ion-Mobility Mass Spectrometry for the Rapid Determination of the Topology of Interlocked and Knotted Molecules. *Angew. Chem. - Int. Ed.* **2019**, *58* (33), 11324–11328. <https://doi.org/10.1002/anie.201904541>.
- (27) Geue, N.; Bennett, T. S.; Arama, A. A.; Ramakers, L. A. I.; Whitehead, G. F. S.; Timco, G. A.; Armentrout, P. B.; McInnes, E. J. L.; Burton, N. A.; Winpenny, R. E. P.; Barran, P. E. Disassembly Mechanisms and Energetics of Polymetallic Rings and Rotaxanes. *J. Am. Chem. Soc.* **2022**, *144* (49), 22528–22539. <https://doi.org/10.1021/jacs.2c07522>.
- (28) Huang, Z.; Yao, Y.-N.; Li, W.; Hu, B. Analytical Properties of Electrospray Ionization Mass Spectrometry with Solid Substrates and Nonpolar Solvents. *Anal. Chim. Acta* **2019**, *1050*, 105–112. <https://doi.org/10.1016/j.aca.2018.10.064>.
- (29) Konermann, L. Addressing a Common Misconception: Ammonium Acetate as Neutral pH “Buffer” for Native Electrospray Mass Spectrometry. *J. Am. Soc. Mass Spectrom.* **2017**, *28* (9), 1827–1835. <https://doi.org/10.1007/s13361-017-1739-3>.

- (30) Li, C.; Chu, S.; Tan, S.; Yin, X.; Jiang, Y.; Dai, X.; Gong, X.; Fang, X.; Tian, D. Towards Higher Sensitivity of Mass Spectrometry: A Perspective From the Mass Analyzers. *Front. Chem.* **2021**, *9*. <https://doi.org/10.3389/fchem.2021.813359/full>.
- (31) Huang, Y.; Zhang, Q.; Liu, Y.; Jiang, B.; Xie, J.; Gong, T.; Jia, B.; Liu, X.; Yao, J.; Cao, W.; Shen, H.; Yang, P. Aperture-Controllable Nano-Electrospray Emitter and Its Application in Cardiac Proteome Analysis. *Talanta* **2020**, *207*, 120340. <https://doi.org/10.1016/j.talanta.2019.120340>.
- (32) Chen, S.; Zeng, J.; Zhang, Z.; Xu, B.; Zhang, B. Recent Advancements in Nanoelectrospray Ionization Interface and Coupled Devices. *J. Chromatogr. Open* **2022**, *2*, 100064. <https://doi.org/10.1016/j.jcoa.2022.100064>.
- (33) Cox, K. A.; Cleven, C. D.; Cooks, R. G. Mass Shifts and Local Space Charge Effects Observed in the Quadrupole Ion Trap at Higher Resolution. *Int. J. Mass Spectrom. Ion Process.* **1995**, *144* (1), 47–65. [https://doi.org/10.1016/0168-1176\(95\)04152-B](https://doi.org/10.1016/0168-1176(95)04152-B).
- (34) Stewart, I. I.; Olesik, J. W. Time-Resolved Measurements with Single Droplet Introduction to Investigate Space-Charge Effects in Plasma Mass Spectrometry. *J. Am. Soc. Mass Spectrom.* **1999**, *10* (2), 159–174. [https://doi.org/10.1016/S1044-0305\(98\)00136-6](https://doi.org/10.1016/S1044-0305(98)00136-6).
- (35) Eldrid, C.; O'Connor, E.; Thalassinos, K. Concentration-Dependent Coulombic Effects in Travelling Wave Ion Mobility Spectrometry Collision Cross Section Calibration. *Rapid Commun. Mass Spectrom.* **2020**, *34* (S4). <https://doi.org/10.1002/rcm.8613>.
- (36) Kwantwi-Barima, P.; Garimella, S. V. B.; Attah, I. K.; Zheng, X.; Ibrahim, Y. M.; Smith, R. D. Accumulation of Large Ion Populations with High Ion Densities and Effects Due to Space Charge in Traveling Wave-Based Structures for Lossless Ion Manipulations (SLIM) IMS-MS. *J. Am. Soc. Mass Spectrom.* **2024**, *35* (2), 365–377. <https://doi.org/10.1021/jasms.3c00389>.
- (37) Wei, A. A. J.; Joshi, A.; Chen, Y.; McIndoe, J. S. Strategies for Avoiding Saturation Effects in ESI-MS. *Int. J. Mass Spectrom.* **2020**, *450*, 116306. <https://doi.org/10.1016/j.ijms.2020.116306>.
- (38) *The Nobel Prize in Chemistry 2002*. NobelPrize.org. <https://www.nobelprize.org/prizes/chemistry/2002/summary/> (accessed 2024-01-16).
- (39) Konermann, L.; Ahadi, E.; Rodriguez, A. D.; Vahidi, S. Unraveling the Mechanism of Electrospray Ionization. *Anal. Chem.* **2013**, *85*, 2–9. <https://doi.org/10.1109/CDC.2015.7402330>.
- (40) Konermann, L.; Haidar, Y. Mechanism of Magic Number NaCl Cluster Formation from Electrosprayed Water Nanodroplets. *Anal. Chem.* **2022**, *94* (47), 16491–16501. <https://doi.org/10.1021/acs.analchem.2c04141>.
- (41) Khristenko, N.; Rosu, F.; Largy, E.; Haustant, J.; Mesmin, C.; Gabelica, V. Native Electrospray Ionization of Multi-Domain Proteins via a Bead Ejection Mechanism. *J. Am. Chem. Soc.* **2023**, *145* (1), 498–506. <https://doi.org/10.1021/jacs.2c10762>.
- (42) Karas, M.; Bahr, U.; Dülcks, T. Nano-Electrospray Ionization Mass Spectrometry: Addressing Analytical Problems beyond Routine. *Fresenius J. Anal. Chem.* **2000**, *366* (6), 669–676. <https://doi.org/10.1007/s002160051561>.
- (43) Jordan, J. S.; Xia, Z.; Williams, E. R. Tips on Making Tiny Tips: Secrets to Submicron Nanoelectrospray Emitters. *J. Am. Soc. Mass Spectrom.* **2022**, *33* (3), 607–611. <https://doi.org/10.1021/jasms.1c00372>.

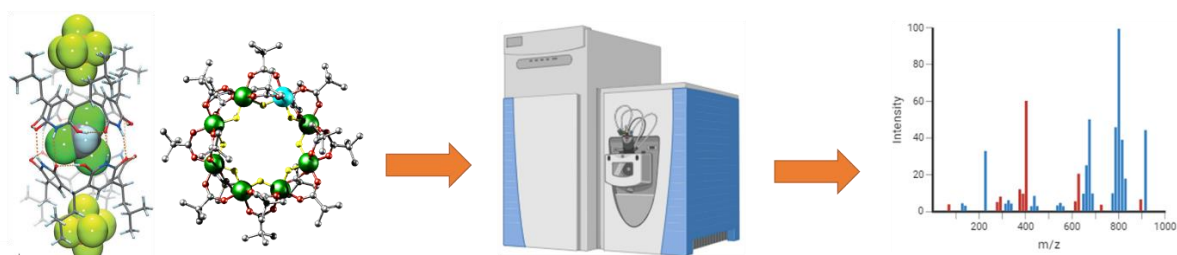
- (44) Wörner, T. P.; Shamorkina, T. M.; Snijder, J.; Heck, A. J. R. Mass Spectrometry-Based Structural Virology. *Anal. Chem.* **2021**, *93* (1), 620–640. <https://doi.org/10.1021/acs.analchem.0c04339>.
- (45) Jordan, J. S.; Miller, Z. M.; Harper, C. C.; Hanozin, E.; Williams, E. R. Lighting Up at High Potential: Effects of Voltage and Emitter Size in Nanoelectrospray Ionization. *J. Am. Soc. Mass Spectrom.* **2023**, *34* (6), 1186–1195. <https://doi.org/10.1021/jasms.3c00121>.
- (46) Kirshenbaum, N.; Michaelievski, I.; Sharon, M. Analyzing Large Protein Complexes by Structural Mass Spectrometry. *JoVE J. Vis. Exp.* **2010**, No. 40, e1954. <https://doi.org/10.3791/1954>.
- (47) Du, C. *Setting up a nanospray emitter into the MS source head*. <https://nativems.osu.edu/sites/default/files/2022-08/NanosprayEmitter.pdf>.
- (48) Sanders, K. L.; Edwards, J. L. Nano-Liquid Chromatography-Mass Spectrometry and Recent Applications in Omics Investigations. *Anal. Methods* **2020**, *12* (36), 4404–4417. <https://doi.org/10.1039/D0AY01194K>.
- (49) Daub, C. D.; Cann, N. M. How Are Completely Desolvated Ions Produced in Electrospray Ionization: Insights from Molecular Dynamics Simulations. *Anal. Chem.* **2011**, *83* (22), 8372–8376. <https://doi.org/10.1021/ac202103p>.
- (50) Suzuki, K.; Tominaga, M.; Kawano, M.; Fujita, M. Self-Assembly of an M6L12 Coordination Cube. *Chem. Commun.* **2009**, No. 13, 1638–1640. <https://doi.org/10.1039/B822311D>.
- (51) Wilson, E. F.; Abbas, H.; Duncombe, B. J.; Streb, C.; Long, D.-L.; Cronin, L. Probing the Self-Assembly of Inorganic Cluster Architectures in Solution with Cryospray Mass Spectrometry: Growth of Polyoxomolybdate Clusters and Polymers Mediated by Silver(I) Ions. *J. Am. Chem. Soc.* **2008**, *130* (42), 13876–13884. <https://doi.org/10.1021/ja802514q>.
- (52) Vilà-Nadal, L.; Rodríguez-Forteza, A.; Yan, L.-K.; Wilson, E. F.; Cronin, L.; Poblet, J. M. Nucleation Mechanisms of Molecular Oxides: A Study of the Assembly–Disassembly of [W6O19]2– by Theory and Mass Spectrometry. *Angew. Chem. Int. Ed.* **2009**, *48* (30), 5452–5456. <https://doi.org/10.1002/anie.200901348>.
- (53) Yamaguchi, K. Cold-Spray Ionization Mass Spectrometry: Principle and Applications. *J. Mass Spectrom.* **2003**, *38* (5), 473–490. <https://doi.org/10.1002/jms.488>.
- (54) Miras, H. N.; Cronin, L. Electrospray and Cryospray Mass Spectrometry: From Serendipity to Designed Synthesis of Supramolecular Coordination and Polyoxometalate Clusters. In *New Strategies in Chemical Synthesis and Catalysis*; John Wiley & Sons, Ltd, 2012; pp 1–32. <https://doi.org/10.1002/9783527645824.ch1>.
- (55) Montaudo, G.; Samperi, F.; Montaudo, M. S. Characterization of Synthetic Polymers by MALDI-MS. *Prog. Polym. Sci.* **2006**, *31* (3), 277–357. <https://doi.org/10.1016/j.progpolymsci.2005.12.001>.
- (56) Baytekin, B.; Werner, N.; Luppertz, F.; Engeser, M.; Brüggemann, J.; Bitter, S.; Henkel, R.; Felder, T.; Schalley, C. A. How Useful Is Mass Spectrometry for the Characterization of Dendrimers?: “Fake Defects” in the ESI and MALDI Mass Spectra of Dendritic Compounds. *Int. J. Mass Spectrom.* **2006**, *249–250*, 138–148. <https://doi.org/10.1016/j.ijms.2006.01.016>.
- (57) Lu, I.-C.; Lee, C.; Lee, Y.-T.; Ni, C.-K. Ionization Mechanism of Matrix-Assisted Laser Desorption/Ionization. *Annu. Rev. Anal. Chem.* **2015**, *8* (1), 21–39. <https://doi.org/10.1146/annurev-anchem-071114-040315>.

- (58) Vikse, K. L.; Scott McIndoe, J. Ionization Methods for the Mass Spectrometry of Organometallic Compounds. *J. Mass Spectrom.* **2018**, *53* (10), 1026–1034. <https://doi.org/10.1002/jms.4286>.
- (59) Kelly, R. T.; Tolmachev, A. V.; Page, J. S.; Tang, K.; Smith, R. D. The Ion Funnel: Theory, Implementations, and Applications. *Mass Spectrom. Rev.* **2010**, *29* (2), 294–312. <https://doi.org/10.1002/mas.20232>.
- (60) Liigand, P.; Kaupmees, K.; Haav, K.; Liigand, J.; Leito, I.; Girod, M.; Antoine, R.; Kruve, A. Think Negative: Finding the Best Electrospray Ionization/MS Mode for Your Analyte. *Anal. Chem.* **2017**, *89* (11), 5665–5668. <https://doi.org/10.1021/acs.analchem.7b00096>.
- (61) Eliuk, S.; Makarov, A. Evolution of Orbitrap Mass Spectrometry Instrumentation. *Annu. Rev. Anal. Chem.* **2015**, *8* (1), 61–80. <https://doi.org/10.1146/annurev-anchem-071114-040325>.
- (62) Marty, M. T.; Baldwin, A. J.; Marklund, E. G.; Hochberg, G. K. A.; Benesch, J. L. P.; Robinson, C. V. Bayesian Deconvolution of Mass and Ion Mobility Spectra: From Binary Interactions to Polydisperse Ensembles. *Anal. Chem.* **2015**, *87* (8), 4370–4376. <https://doi.org/10.1021/acs.analchem.5b00140>.
- (63) *enviPat: isotope pattern calculator*. <https://www.envipat.eawag.ch/index.php> (accessed 2024-01-18).
- (64) Geue, N.; Timco, G. A.; Whitehead, G. F. S.; McInnes, E. J. L.; Burton, N. A.; Winpenny, R. E. P.; Barran, P. E. Formation and Characterization of Polymetallic {Cr<sub>x</sub>My} Rings in Vacuo. *Nat. Synth.* **2023**, *2* (10), 926–936.
- (65) Cooper-Shepherd, D. A.; Wildgoose, J.; Kozlov, B.; Johnson, W. J.; Tyldesley-worster, R.; Palmer, M. E.; Hoyes, J. B.; Mccullagh, M.; Jones, E.; Tonge, R.; Marsden-edwards, E.; Nixon, P.; Verenchikov, A.; Langridge, J. I. Novel Hybrid Quadrupole-Multireflecting Time-of-Flight Mass Spectrometry System. *J. Am. Soc. Mass Spectrom. Spectrom.* **2023**, *34* (2), 264–272. <https://doi.org/10.1021/jasms.2c00281>.
- (66) Stewart, H. I.; Grinfeld, D.; Giannakopoulos, A.; Petzoldt, J.; Shanley, T.; Garland, M.; Denisov, E.; Peterson, A. C.; Damoc, E.; Zeller, M.; Arrey, T. N.; Pashkova, A.; Renuse, S.; Hakimi, A.; Kühn, A.; Biel, M.; Kreuzmann, A.; Hagedorn, B.; Colonius, I.; Schütz, A.; Stefes, A.; Dwivedi, A.; Mourad, D.; Hoek, M.; Reitemeier, B.; Cochems, P.; Kholomeev, A.; Ostermann, R.; Quiring, G.; Ochmann, M.; Möhring, S.; Wagner, A.; Petker, A.; Kanngiesser, S.; Wiedemeyer, M.; Balschun, W.; Hermanson, D.; Zabrouskov, V.; Makarov, A. A.; Hock, C. Parallelized Acquisition of Orbitrap and Astral Analyzers Enables High-Throughput Quantitative Analysis. *Anal. Chem.* **2023**, *95* (42), 15656–15664. <https://doi.org/10.1021/acs.analchem.3c02856>.
- (67) *Isotope Distribution Calculator, Mass Spec Plotter, Isotope Abundance Graphs*. <https://www.sisweb.com/mstools/isotope.htm> (accessed 2024-01-18).
- (68) *ChemCalc: molecular formula information*. <https://www.chemcalc.org/?ionizations=&mf=> (accessed 2024-02-14).
- (69) Loos, M.; Gerber, C.; Corona, F.; Hollender, J.; Singer, H. Accelerated Isotope Fine Structure Calculation Using Pruned Transition Trees. *Anal. Chem.* **2015**, *87* (11), 5738–5744. <https://doi.org/10.1021/acs.analchem.5b00941>.
- (70) Sawada, M.; Takai, Y.; Kaneda, T.; Arakawa, R.; Okamoto, M.; Doe, H.; Matsuo, T.; Naemura, K.; Hirose, K.; Tobe, Y. Chiral Molecular Recognition in Electrospray Ionization Mass Spectrometry. *Chem. Commun.* **1996**, No. 15, 1735–1736. <https://doi.org/10.1039/cc9960001735>.

- (71) De Vijlder, T.; Valkenburg, D.; Lemièrre, F.; Romijn, E. P.; Laukens, K.; Cuyckens, F. A Tutorial in Small Molecule Identification via Electrospray Ionization-Mass Spectrometry: The Practical Art of Structural Elucidation. *Mass Spectrom. Rev.* **2018**, *37* (5), 607–629. <https://doi.org/10.1002/mas.21551>.
- (72) Yunker, L. P. E.; Donneck, S.; Ting, M.; Yeung, D.; McIndoe, J. S. PythoMS: A Python Framework To Simplify and Assist in the Processing and Interpretation of Mass Spectrometric Data. *J. Chem. Inf. Model.* **2019**, *59* (4), 1295–1300. <https://doi.org/10.1021/acs.jcim.9b00055>.
- (73) Bayat, P.; Lesage, D.; Cole, R. B. Tutorial: Ion Activation in Tandem Mass Spectrometry Using Ultra-High Resolution Instrumentation. *Mass Spectrom. Rev.* **2020**, *39* (5–6), 680–702. <https://doi.org/10.1002/mas.21623>.
- (74) Grabarics, M.; Lettow, M.; Kirschbaum, C.; Greis, K.; Manz, C.; Pagel, K. Mass Spectrometry-Based Techniques to Elucidate the Sugar Code. *Chem. Rev.* **2022**, *122* (8), 7840–7908. <https://doi.org/10.1021/acs.chemrev.1c00380>.
- (75) McLafferty, F. W. Mass Spectrometric Analysis. Molecular Rearrangements. *Anal. Chem.* **1959**, *31* (1), 82–87. <https://doi.org/10.1021/ac60145a015>.
- (76) Steckel, A.; Schlosser, G. An Organic Chemist's Guide to Electrospray Mass Spectrometric Structure Elucidation. *Molecules* **2019**, *24* (3), 611. <https://doi.org/10.3390/molecules24030611>.
- (77) Chakraborty, P.; Baksi, A.; Khatun, E.; Nag, A.; Ghosh, A.; Pradeep, T. Dissociation of Gas Phase Ions of Atomically Precise Silver Clusters Reflects Their Solution Phase Stability. *J. Phys. Chem. C* **2017**, *121* (20), 10971–10981. <https://doi.org/10.1021/acs.jpcc.6b12485>.
- (78) Bennett, T.; Geue, N.; Timco, G.; Whitehead, G.; Vitorica-Yrezabal, I.; Barran, P.; McInnes, E.; Winpenny, R. Studying Cation Exchange in {Cr7Co} Pseudorotaxanes: Preparatory Studies for Making Hybrid Molecular Machines. ChemRxiv December 18, 2023. <https://doi.org/10.26434/chemrxiv-2023-bc339>.
- (79) Armentrout, P. B. The Power of Accurate Energetics (or Thermochemistry: What Is It Good For?). *J. Am. Soc. Mass Spectrom.* **2013**, *24* (2), 173–185. <https://doi.org/10.1007/s13361-012-0515-7>.
- (80) Geue, N.; Winpenny, R. E. P.; Barran, P. Ion Mobility Mass Spectrometry for Synthetic Molecules: Expanding the Analytical Toolbox. ChemRxiv January 10, 2024. <https://doi.org/10.26434/chemrxiv-2024-g7swp>.
- (81) Fort, K. L.; Van De Waterbeemd, M.; Boll, D.; Reinhardt-Szyba, M.; Belov, M. E.; Sasaki, E.; Zschoche, R.; Hilvert, D.; Makarov, A. A.; Heck, A. J. R. Expanding the Structural Analysis Capabilities on an Orbitrap-Based Mass Spectrometer for Large Macromolecular Complexes. *Analyst* **2018**, *143* (1), 100–105. <https://doi.org/10.1039/c7an01629h>.
- (82) Bell, D. J.; Zhang, T.; Geue, N.; Rogers, C. J.; Barran, P. E.; Bowen, A. M.; Natrajan, L. S.; Riddell, I. A. Hexanuclear Ln6L6 Complex Formation by Using an Unsymmetric Ligand. *Chem. - Eur. J.* **2023**, *29* (71), e202302497. <https://doi.org/10.1002/chem.202302497>.
- (83) Giles, K.; Pringle, S. D.; Worthington, K. R.; Little, D.; Wildgoose, J. L.; Bateman, R. H. Applications of a Travelling Wave-Based Radio-Frequency-Only Stacked Ring Ion Guide. *Rapid Commun. Mass Spectrom.* **2004**, *18* (20), 2401–2414. <https://doi.org/10.1002/rcm.1641>.
- (84) Pringle, S. D.; Giles, K.; Wildgoose, J. L.; Williams, J. P.; Slade, S. E.; Thalassinou, K.; Bateman, R. H.; Bowers, M. T.; Scrivens, J. H. An Investigation of the Mobility

- Separation of Some Peptide and Protein Ions Using a New Hybrid Quadrupole/Travelling Wave IMS/Oa-ToF Instrument. *Int. J. Mass Spectrom.* **2007**, *261* (1), 1–12. <https://doi.org/10.1016/j.ijms.2006.07.021>.
- (85) Christofi, E.; Barran, P. Ion Mobility Mass Spectrometry (IM-MS) for Structural Biology: Insights Gained by Measuring Mass, Charge, and Collision Cross Section. *Chem. Rev.* **2023**, *123* (6), 2902–2949. <https://doi.org/10.1021/acs.chemrev.2c00600>.
- (86) von Helden, G.; Gotts, N. G.; Bowers, M. T. Experimental Evidence for the Formation of Fullerenes by Collisional Heating of Carbon Rings in the Gas Phase. *Nature* **1993**, *363* (6424), 60–63. <https://doi.org/10.1038/363060a0>.
- (87) Hunter, J.; Fye, J.; Jarrold, M. F. Annealing C60+: Synthesis of Fullerenes and Large Carbon Rings. *Science* **1993**, *260* (5109), 784–786. <https://doi.org/10.1126/science.260.5109.784>.
- (88) Geue, N.; Bennett, T. S.; Ramakers, L. A. I.; Timco, G. A.; McInnes, E. J. L.; Burton, N. A.; Armentrout, P. B.; Winpenny, R. E. P.; Barran, P. E. Adduct Ions as Diagnostic Probes of Metallosupramolecular Complexes Using Ion Mobility Mass Spectrometry. *Inorg. Chem.* **2023**, *62* (6), 2672–2679. <https://doi.org/10.1021/acs.inorgchem.2c03698>.
- (89) Ballesteros, B.; Faust, T. B.; Lee, C. F.; Leigh, D. A.; Muryn, C. A.; Pritchard, R. G.; Schultz, D.; Teat, S. J.; Timco, G. A.; Winpenny, R. E. P. Synthesis, Structure, and Dynamic Properties of Hybrid Organic-Inorganic Rotaxanes. *J. Am. Chem. Soc.* **2010**, *132* (43), 15435–15444. <https://doi.org/10.1021/ja1074773>.
- (90) Giles, K.; Ujma, J.; Wildgoose, J.; Pringle, S.; Richardson, K.; Langridge, D.; Green, M. A. Cyclic Ion Mobility-Mass Spectrometry System. *Anal. Chem.* **2019**, *91* (13), 8564–8573. <https://doi.org/10.1021/acs.analchem.9b01838>.
- (91) Greis, K.; Kirschbaum, C.; von Helden, G.; Pagel, K. Gas-Phase Infrared Spectroscopy of Glycans and Glycoconjugates. *Curr. Opin. Struct. Biol.* **2022**, *72*, 194–202. <https://doi.org/10.1016/j.sbi.2021.11.006>.
- (92) Anggara, K.; Sršan, L.; Jaroentomeechai, T.; Wu, X.; Rauschenbach, S.; Narimatsu, Y.; Clausen, H.; Ziegler, T.; Miller, R. L.; Kern, K. Direct Observation of Glycans Bonded to Proteins and Lipids at the Single-Molecule Level. *Science* **2023**, *382* (6667), 219–223. <https://doi.org/10.1126/science.adh3856>.

**For Table of Contents only:**



Mass spectrometry is ideally suitable to characterise supramolecules and coordination compounds, and this tutorial discusses sample preparation, technical details, data analysis and interpretation as well as two-dimensional gas phase separation approaches.